CHIN. PHYS. LETT. Vol. 34, No. 7 (2017) 077203

BiPh-*m*-BiDPO as a Hole-Blocking Layer for Organic Light-Emitting Diodes: Revealing Molecular Structure-Properties Relationship *

Ning-Ning Chen(陈宁宁), Wan-Yi Tan(谭婉怡), Dong-Yu Gao(高栋雨), Jian-Hua Zou(邹建华), Jun-Zhe Liu(刘俊哲), Jun-Biao Peng(彭俊彪), Yong Cao(曹镛), Xu-Hui Zhu(朱旭辉)**

State Key Laboratory of Luminescent Materials and Devices, and Institute of Polymer & Optoelectronic Materials and Devices, South China University of Technology, Guangzhou 510640

(Received 24 April 2017)

We report a simple hole-blocking material (biphenyl-3,3'-diyl)bis(diphenylphosphine oxide) (BiPh-m-BiDPO) based on our recent advance. The bis(phosphine oxide) compound shows HOMO/LUMO levels of ∼−6.71/ − 2.51 eV. Its phosphorescent spectrum in a solid film features two major emission bands peaking at 2.69 and 2.4 eV, corresponding to 0–0 and 0–1 vibronic transitions, respectively. The measurement of the electron-only devices reveals that BiPh-m-BiDPO possesses electron mobility of 2.28×10^{-9}–3.22×10^{-8} $cm^2V^{-1}s^{-1}$ *at* $E = 2$–5×10^5 V/cm. *The characterization of the sky blue fluorescent and red phosphorescent pin organic light-emitting diodes (OLEDs) utilizing BiPh-m-BiDPO as the hole blocker shows that its shallow LUMO level as well as the low electron mobility affects significantly the power efficiency and hence operational stability, relative to the luminous efficiency, especially at high luminance. In combination with our recent results, the present study provides an indepth insight on the molecular structure-property correlation in the organic phosphinyl-containing hole-blocking materials.*

PACS: 72.80.Le, 78.60.Fi, 85.60.Jb DOI: 10.1088/0256-307X/34/7/077203

Organic phosphinyl-containing optoelectronic materials are widely utilized as emitters, hosts, and electron transport/hole-blocking materials in organic light-emitting diodes (OLEDs) and also as cathode interfacial materials in organic photovoltaics (OPVs).[1−18] Up to now, there have appeared very few studies concerning their function to afford stable OLEDs. The early results showed that the organic phosphinyl compounds may encounter morphological instability[3] or potential chemical instabilities in the operating devices.[19]

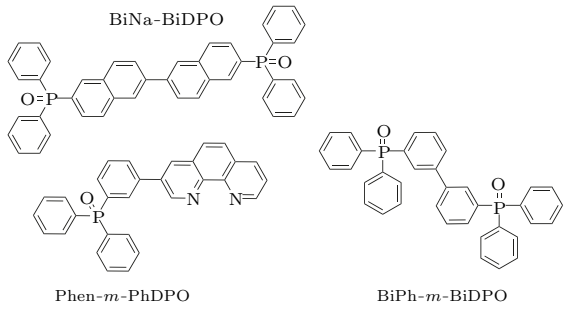

Fig. 1. Chemical structures of BiNa-BiDPO, Phen-*m*-PhDPO and BiPh-*m*-BiDPO.

Recently, we have developed a series of phosphinyl-containing organic electron-transport/hole-blocking materials, for instance (2,2'-binaphthyl-6,6'-diyl)bis(diphenylphosphine oxide) (BiNa-BiDPO) and 3-(6-diphenylphosphinylnaphth-2-yl)-1,10-phenanthroline (Phen-*m*-PhDPO) (Fig. 1), which provide promising OLED stability.[20,21]

In this Letter, we report a simple compound (biphenyl-3,3'-diyl)bis(diphenylphosphine oxide) (BiPh-*m*-BiDPO) as a hole blocker with the twisted chemical structure to increase the triplet energy, in comparison with BiNa-BiDPO. BiPh-*m*-BiDPO is investigated in sky blue fluorescent and green, red phosphorescent OLEDs. In comparison with BiNa-BiDPO and Phen-*m*-PhDPO, the present study will serve as a helpful guide for designing organic electron-transport/hole-blocking materials.

The synthesis of BiPh-*m*-BiDPO as well as chemical, thermal and optical characterizations was in accordance with BiNa-BiDPO and Phen-*m*-PhDPO:[20,21] ^{1}H NMR (400 MHz, DMSO, ppm): δ 7.88 (d, 2H), 7.75 (d, 2H), 7.62 (m, 24H). Anal. Calcd. for $C_{36}H_{30}O_3P_2$(M+H_2O): C, 75.52; H, 5.28. Found: C, 75.40; H, 5.003. MS (APCI) m/z: $(M+H)^+$ calcd. for $C_{36}H_{29}O_2P_2$, 555.16; found, 555.1. BiPh-*m*-BiDPO was studied as a hole-blocking layer in the thermally deposited sky-blue fluorescent OLEDs (FLOLEDs), green and red phosphorescent OLEDs (PHOLEDs), respectively. Indium tin oxide (ITO, 15 Ωsquare^{-1})-coated glass substrates were cleaned with distilled water, acetone, detergent, distilled water and 2-propanol in an ultrasonic bath before device fabrication. Afterward, all the organic and metal layers were deposited in turn. During the deposition, the base pressure of the chamber was maintained lower than 2×10^{-7} Torr. In the deposition of the doping layers, deposition rates of both host and guest were controlled by their correspondingly independent quartz crystal oscillators. The devices were encapsulated immediately after preparation under a nitrogen atmosphere using epoxy glue and glass lids. The emission area of the devices was 0.09 cm^2, as determined from the overlap area of the anode and the cath-

*Supported by the National Natural Science Foundation of China under Grant No U1301243, and the National Key Research and Development Program of China under Grant No 2016YFB0400701.

**Corresponding author. Email: xuhuizhu@scut.edu.cn

© 2017 Chinese Physical Society and IOP Publishing Ltd

ode. The electroluminescent (EL) spectra, the current density (J)-voltage (V)-luminance (L) characteristics were recorded simultaneously, using a computer-controlled source meter (Keithley 2400) and a multimeter (Keithley 2000) with a calibrated silicon photodiode. All the measurements were carried out at room temperature under ambient conditions.

A single carrier electron-only device (ITO/BPhen: Cs_2CO_3(20 nm)/HBL(150 nm)/BPhen: Cs_2CO_3 (20 nm)/Al(200 nm)) was fabricated to measure the electron mobility of BiPh-*m*-BiDPO.

Ultraviolet photoemission spectroscopy (UPS) measurement was carried out using a Thermo Scientific ESCALAB 250 surface analysis system. A helium discharge UV lamp with the energy of 21.2 eV (He I) was used as the source of UV light. The vacuum level was determined from UPS spectra at the lowkinetic energy onset (secondary electron cutoff) with −5 V sample bias. The ITO substrate was cleaned by subsequent sonication in acetone, isopropyl alcohol and deionized water before being loaded into the chamber. BiPh-*m*-BiDPO was deposited on ITO by thermal evaporation at a growth rate of 0.2 Ås^{-1} in a vacuum lower than 5×10^{-4} Pa.

It is interesting to note that like some other bis(diphenylphosphine oxide) compounds, such as (spiro[fluorene-9,9'-xanthene]-2,7-diylbis(diphenylphosphine oxide) (SFX27PO[14]) and BiNa- BiDPO,[20] BiPh-*m*-BiDPO has a high tendency to include one H_2O molecule in the ambient, based on the microanalysis data. Nevertheless, we need to point out that the crystalline compound (naphth-2,6-diyl)bis(diphenylphosphine oxide) (NaBDPO[15]) as well as (9,9-dimethylfluorene-2,7-diyl)bis(diphenylphosphine oxide)[22] possesses no water or organic solvent, while spiro[fluorene-9,9'-xanthene]-2',7'-diylbis(diphenylphosphine oxide) (SFX2'7'PO) holds two CH_2Cl_2 molecules, confirmed by x-ray single crystallography.[14]

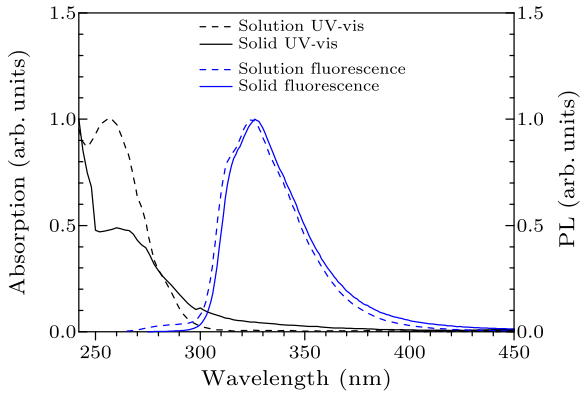

Fig. 2. Normalized UV-vis and fluorescence spectra of BiPh-*m*-BiDPO in CH_2Cl_2 ($\sim 1.0 \times 10^{-5}$ molL^{-1}) and as films on quartz glass. The fluorescence spectra were recorded under excitation wavelength of 330 nm.

Based on the absorption edge of the solid film, the optical bandgap of BiPh-*m*-BiDPO is calculated to be ∼4.2 eV (Fig. 2). Its film exhibits a fluorescent emission maximum at 326 nm. As is expected, BiPh-*m*-BiDPO shows an increasing triplet energy (E_T) in solid state, compared with BiNa-BiDPO (Fig. 3), benefiting from its twisted molecular structure incorporating 1,3-phenylene as the linkage. Specifically, BiPh-*m*-BiDPO shows two major vibronic emission peaks at about 460 nm ($T_{0-0} \approx 2.69$ eV) and 515 nm ($T_{0-1} \approx 2.40$ eV), respectively, in contrast with an emission maximum at 560 nm ($T \approx 2.21$ eV) for BiNaBiDPO.[20,21]

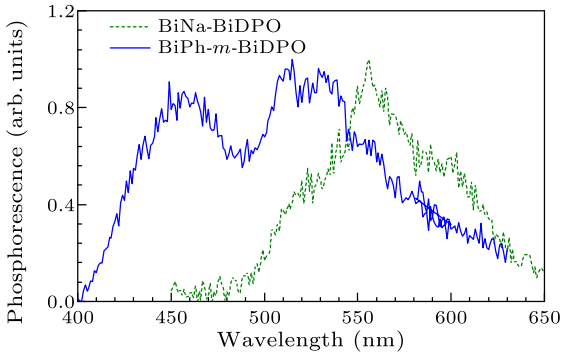

Fig. 3. Normalized phosphorescence spectra of BiPh-*m*-BiDPO and BiNa-BiDPO[20,21] as neat films recorded at 77 K.

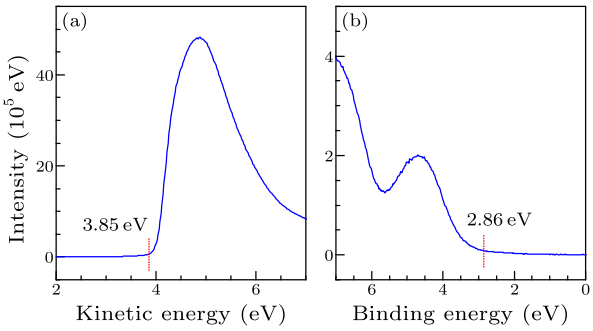

Fig. 4. (a) UPS spectra at the low-kinetic energy part and (b) valence band spectra near the Fermi level for BiPh-*m*-BiDPO (10 nm) on the ITO surface.

BiPh-*m*-BiDPO is thermally stable up to about 310℃. Differential scanning calorimetry (DSC) measurements reveal a melting point of 226℃ in the first heating run. Neither crystallization upon cooling nor remelting is observed. Instead, a distinct glass transition is evidenced at ca. 80℃ during the reheating process.

The UPS measurement was carried out on a thin film of BiPh-*m*-BiDPO (10 nm) on ITO, revealing that it possesses a deep HOMO level of −6.71 eV (Fig. 4). Consequently, the LUMO level is calculated to be −2.51 eV, based on its HOMO level and optical bandgap of ∼4.2 eV. By contrast, BiNa-BiDPO shows an increasing HOMO level of −6.12 eV with a reduction of the LUMO level of −2.77 eV, in good agreement with its enhanced conjugated structure.[20]

BiPh-*m*-BiDPO was evaluated as a hole-blocking layer in thermally deposited pin sky-blue fluorescent OLED (FLOLED), green and red phosphorescent OLEDs (PHOLEDs). The chemical struc-

tures of the charge transport materials and individual host/emitting materials in the blue sky, green and red emitting layers as well as the p-dopant F4-TCNQ are presented in Fig. 5 together with the HOMO/LUMO levels. The OLED structures are shown as follows: sky blue FLOLED: ITO/MeOTPD: F4TCNQ (100 nm, 4%)/NPB (20 nm)/MADN: DSAPh (30 nm, 7%)/BiPh-*m*-BiDPO (10 nm)/BPhen: Cs_2CO_3 (20 nm, 50%)/Al, where MeO-TPD=*N*, *N*, *N*′, *N*′-tetra(4-methoxyphenyl)-[1,1'-biphenyl]-4,4'-diamine, F4-TCNQ=tetrafluorotetracyanoquino-dimethane, NPB=4,4'-bis((1-naphthyl)phenylamino)biphenyl, MADN=2-methyl-9,10-di(2-naphthyl)anthracene, DSA-Ph=*p*-bis(*p*−*N*, *N*-diphenylaminostyryl)benzene, and BPhen=4,7-diphenyl-1,10-phenanthroline. Green PHOLED: ITO/MeOTPD: F4TCNQ (100 nm, 4%)/NPB (15 nm)/TCTA (5 nm)/$Bepp_2$: $Ir(ppy)_3$ (30 nm, 9%)/BiPh-*m*-BiDPO (10 nm)/BPhen: Cs_2CO_3 (20 nm, 50%)/Al, where TCTA=4,4',4"-tris(*N*-carbazolyl)triphenylamine, $Bepp_2$=bis(2-(2-hydroxyphenyl)pyridine)beryllium, and $Ir(ppy)_3$=tris(2-phenylpyridine)iridium. Red PHOLED: ITO/MeOTPD: F4TCNQ (100 nm, 4%)/NPB (20 nm)/$Bebq_2$: $Ir(MDQ)_2(acac)$ (40 nm, 5%)/BiPh-*m*-BiDPO (10 nm)/BPhen: Cs_2CO_3 (20 nm, 50%)/Al, where $Bebq_2$=bis(10-hydroxybenzo[*h*]quinoline)beryllium and $Ir(MDQ)_2(acac)$=bis(2-methyldibenzo-[*f*, *h*]quinoxaline)(acetylacetonate)iridium.

At a luminance of ca. 1000 cdm^{-2}, a luminous efficiency (LE) of 11.3 cdA^{-1} and power efficiency (PE) of 6.3 lmW^{-1} are found for the sky-blue pin FLOLED, 43.4 cdA^{-1} and 24.4 lmW^{-1} for the green PHOLED, and 12.6 cdA^{-1} and 7.3 lmW^{-1} for the red PHOLED, respectively (Figs. 6(a)–6(c) and Table 1). The EL spectra are characteristics of the sky-blue, green and red emitters (Fig. 6(d)).[23–25]

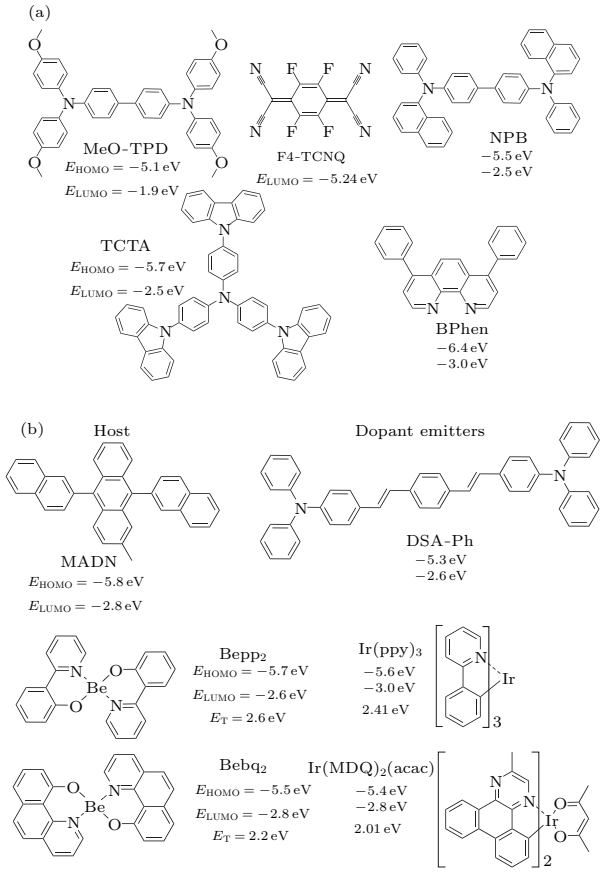

Fig. 5. Chemical structures of charge transport materials as well as the p-dopant F4-TCNQ (a) and host/dopant emitters (b).

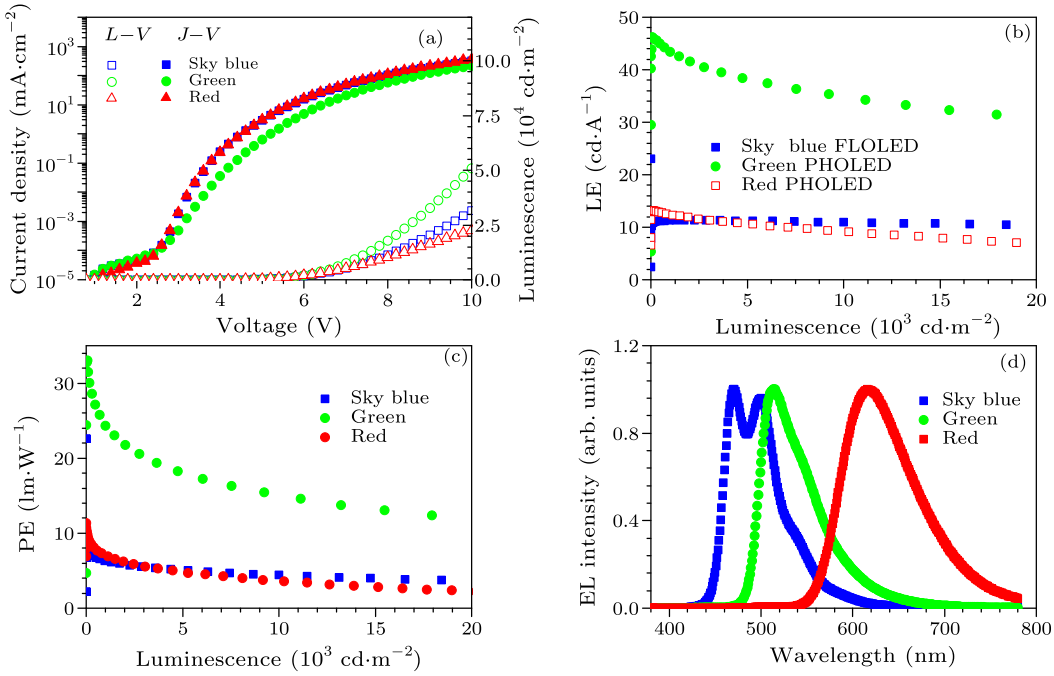

Fig. 6. EL characteristics of the sky blue FLOLED, green and red PHOLEDs: (a) *J*–*V*–*L*, (b) LE–*L*, (c) PE–*L*, and (d) EL spectra.

Table 1. The summary of the OLED characteristics.

OLEDs	V_{on}^{a} (V)	@100 cd/m^2			@1000 cd/m^2		
		LE (cd/A)	PE (lm/W)	V (V)	LE (cd/A)	PE (lm/W)	J (mA/cm^2)
Sky blue FL	3.6	10.9	7.8	5.6	11.3	6.3	8.54
Green PH	3.8	46.1	31.5	5.6	43.4	24.3	2.33
Red PH	3.4	13.2	9.4	5.6	12.3	6.94	9.0

[a]At a luminance of ∼1–4 cd/m^2.

We evaluated the electron mobility (μ_e) of BiPh-*m*-BiDPO in a single carrier device (ITO/BPhen: Cs_2CO_3 (20 nm)/BiPh-*m*-BiDPO (150 nm)/BPhen: Cs_2CO_3 (20 nm)/Al (200 nm)). The current density (J)-voltage (V) characteristics of the electron-only devices are plotted in Fig. 7(a) in a logarithm scale ($\ln(J/E^2)$ versus $\sqrt{E}$), exhibiting a space-charge-limited current (SCLC) behavior at high electric field and can be described by the equation of an SCLC with field-dependent mobility

$$J = \frac{9}{8}\varepsilon\mu(E)\frac{V^2}{d^3} = \frac{9}{8}\varepsilon\mu_0\frac{E^2}{d}\exp(\beta\sqrt{E}), \quad (1)$$

where ε is the permittivity, $\varepsilon = \varepsilon_0\varepsilon_r$ (ε_0 is the permittivity of the free space, and ε_r is the relative permittivity and is assumed to be approximately 3.0), d is the thickness of the active layer, E is the electric field, and $\mu(E)$ is the field-dependent charge carrier mobility and can be expressed by the Poole–Frenkel effect[26]

$$\mu(E) = \mu_0\exp(\beta\sqrt{E}), \quad (2)$$

with μ_0 being the zero-field mobility and β being the field-activation factor of the mobility.

After fitting the $\ln(J/E^2)$–$E^{1/2}$ curve according to Eq. (1), BiPh-*m*-BiDPO exhibited electron mobility of 2.28×10^{-9}–3.22×10^{-8} cm^{2}V^{-1}s^{-1} at $E = 2$–5×10^5 V/cm (Fig. 7(b)). The extracted zero-field electron mobility μ_0 and the field activation factor β of BiPh-*m*-BiDPO were 2.389×10^{-11} cm^{2}V^{-1}s^{-1} and 0.0102 (cm/V)$^{0.5}$. By contrast u_e ≈1.6–8.4 $\times$ 10^{-5} cm^{2}V^{-1}s^{-1} for BiNa-BiDPO[20] and 6.34×10^{-8}–1.58×10^{-6} cm^{2}V^{-1}s^{-1} for Phen-*m*-PhDPO at $E = 2$–5×10^5 V/cm.[21]

Recently, we have reported a triarylphosphine oxide-phenanthroline molecular conjugate (3-(6-diphenylphosphinylnaphth-2-yl)-1, 10-phenanthroline, Phen-*m*-PhDPO, Fig. 1) as a versatile hole-blocking layer for RGB OLEDs.[21] Phen-*m*-PhDPO possesses a deep HOMO/LUMO level of −6.39/−2.9 eV and a major phosphorescent peak at 487 nm (T_{0-1} = 2.54 eV, measured as films at 77 K).[27]

Compared with Phen-*m*-PhDPO, BiPh-*m*-BiDPO exhibited inferior luminous efficiencies at a luminance of ca. 1000 cd/m^2 in the sky blue FLOLED and green/red PHOLEDs. Nevertheless, the resulting power efficiencies were significantly decreased, which is mainly attributed to the inefficient electron injection due to the shallow LUMO level of BiPh-*m*-BiDPO as well as its low electron mobility ($u_e \approx 2.28\times10^{-9}$–$3.22\times10^{-8}$ cm^{2}V^{-1}s^{-1} at $E = 2$–5×10^5 V/cm, See Fig. 7).

Consequently, the OLED stability suffers a considerable loss. For instance, the half lifetime of the green PHOLED is $t_{50} \approx 6.0$ h at ca. 10000 cdm^{-2} versus 39.3 h of the analogue Phen-*m*-PhDPO OLED,[21] driven at a constant current. It is worthwhile pointing out that properly manipulating the organic phosphinyl-containing electron-transport material could afford very long OLED durability with t_{95} of a few hundreds of hours at 1000 cdm^{-2} and the finding shall be reported in due course.

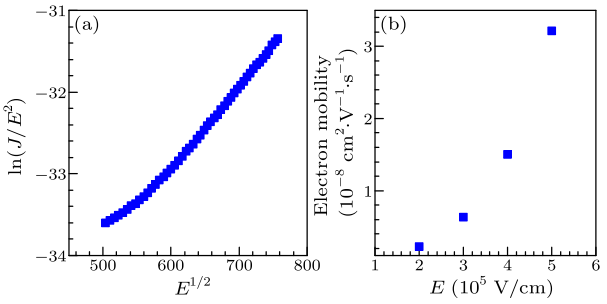

Fig. 7. (a) The $\ln(J/E^2)$–$E^{1/2}$ characteristics of the electron–only devices: ITO/BPhen: Cs_2CO_3 (20 nm)/BiPh-*m*-BiDPO (150 nm)/BPhen: Cs_2CO_3 (20 nm)/Al (200 nm). (b) The corresponding electron mobility versus the applied electric field.

In summary, we have presented a simple organic phosphinyl-containing holeblocking compound BiPh-*m*-BiDPO. Compared with BiNaBiDPO,[20] BiPh-*m*-BiDPO possesses a higher triplet energy while the electron mobility and the LUMO level are compromised. The analysis of the electroluminescent characteristics of sky blue fluorescent and green/red phosphorescent OLEDs involving BiPh-*m*-BiDPO as the hole blocker versus Phen-*m*-PhDPO[21] shows that in addition to the electron mobility, the shallow LUMO level of BiPh-*m*-BiDPO contributes to reducing significantly the power efficiencies rather than the luminous efficiencies. It is worth noting that unlike Phen-*m*-PhDPO, both dry BiPh-*m*-BiDPO and BiNa-BiDPO easily absorb moisture in the ambient, as evidenced from the microanalysis data. The results reported here may provide a useful guide to develop hole-blocking materials for high power efficiency and stable OLEDs.

References

[1] Baumgartner T 2014 *Acc. Chem. Res.* **47** 1613
[2] Oyamada T, Sasabe H, Adachi C et al 2005 *Appl. Phys. Lett.* **86** 033503
[3] Burrows P E, Padmaperuma A B, Sapochak L S et al 2006

Appl. Phys. Lett. **88** 183503
[4] Yin X J, Zhang T K, Peng Q M et al 2015 *J. Mater. Chem. C* **3** 7589
[5] Chien C H, Chen C K, Hsu F M et al 2009 *Adv. Funct. Mater.* **19** 560
[6] Zhou G J, Ho C L, Wong W Y et al 2008 *Adv. Funct. Mater.* **18** 499
[7] Mallesham G M, Swetha C, Niveditha S et al 2015 *J. Mater. Chem. C* **3** 1208
[8] Jiang W, Ye M Y, Ban X X et al 2015 *Dyes Pigm.* **122** 192
[9] Shao S Y, Ding J Q, Ye T L et al 2011 *Adv. Mater.* **23** 3570
[10] Kim B S and Lee J Y 2014 *ACS Appl. Mater. Interfaces* **6** 8396
Jeon S O and Lee J Y 2012 *J. Mater. Chem.* **22** 4233
[11] Wu J, Wu S X, Wu Y et al 2013 *Phys. Chem. Chem. Phys.* **15** 2351
[12] Liu X K, Zheng C J, Lo M F et al 2014 *Chem. Commun.* **50** 2027
[13] Wada A, Yasuda T, Zhang Q et al 2013 *J. Mater. Chem. C* **1** 2404
[14] Han C M, Zhu L P, Li J et al 2014 *Adv. Mater.* **26** 7070
Zhao J, Xie G H, Yin C R et al 2011 *Chem. Mater.* **23** 5331
Tao Y, Xiao J J, Zheng C et al 2013 *Angew. Chem. Int. Ed.* **52** 10491
[15] Tan W Y, Wang R, Li M et al 2014 *Adv. Funct. Mater.* **24** 6540
Ding T, Yang X Y, Ke L et al 2016 *Org. Electron.* **32** 89
Zhang H, Tan W Y, Fladischer S et al 2016 *J. Mater. Chem. A* **4** 5032
[16] Zhuang J Y, Su W M, Wu W C et al 2013 *Tetrahedron* **69** 9038
[17] Jia J L, Zhu L P, Wei Y et al 2015 *J. Mater. Chem. C* **3** 4890
[18] Kan W J, Zhu L P, Wei Y et al 2015 *J. Mater. Chem. C* **3** 5430
[19] Lin N, Qiao J, Duan L et al 2012 *J. Phys. Chem. C* **116** 19451
[20] Tan W Y, Gao D Y, Zhong S et al 2016 *Org. Electron.* **28** 269
[21] Tan W Y, Zou J H, Gao D Y et al 2016 *Adv. Electron. Mater.* **2** 1600101
[22] Padmaperuma A B, Sapochak L S, Burrows and P E 2006 *Chem. Mater.* **18** 2389
Kim D, Salman S, Coropceanu V et al 2010 *Chem. Mater.* **22** 247
[23] Lin M F, Wang L, Wong W K et al 2006 *Appl. Phys. Lett.* **89** 121913
[24] Duan J P, Sun P P and Cheng C H 2003 *Adv. Mater.* **15** 224
[25] Jeon W S, Park T J, Park J J et al 2008 *Appl. Phys. Lett.* **92** 113311
[26] Murgatroyd N 1970 *J. Phys.* D **3** 151
[27] Wei X F, Tan W Y, Zou J H et al 2017 *J. Mater. Chem. C* **5** 2329